Lasers in Medical Science. 2015; 30(2): 891-900

Ultrashort pulsed laser conditioning of human enamel: in vitro study of the influence of geometrical processing parameters on shear bond strength of orthodontic brackets

M. C. Lorenzo , M. Portillo, P. Moreno, J. Montero, A. García, S. E. Santos-del Riego, A. Albaladejo

Abstract
The surfaces of 63 extracted premolar teeth were processed with intense ultrashort laser pulses ($\lambda = 795$ nm; pulse duration, 120 fs; repetition rate, 1 kHz) to produce cross patterns with different pitches (s) in the micrometer range in order to evaluate the influence of such microstructures on the shear bond strengths of orthodontic brackets to enamel. The samples were classified in nine groups corresponding to the control group (raw samples) and eight different laser-processed groups (cross patterns with s increasing from 15 to 180 μm). Brackets were luted with Transbond^{TM} XT adhesive resin to all the samples; after 72 h, they all were submitted to strength test in a universal testing machine. Additionally, a third of the samples underwent morphological analysis of the debonded surface by means of scanning electron microscope microscopy and an analysis of the failure mode based on the adhesive remnant index. The results showed that enamel microstructuring with ultrashort laser pulses remarkably increase the bond strength of brackets. Dense cross patterns ($s < 90$ μm) produce the highest increase of bond strengths as compared to control group whereas light ones ($s > 90$ μm) give rise to smaller improvements of the bond strength. A strong correlation of this behavior with the predominant failure mode in both scenarios was found. So far, the best compromise between suitable adhesive efficiency, processing time minimization, and enamel surface preservation suggests the performance of cross patterns with pitches in the order of 90 μm.

Keywords
Femtosecond laser Enamel Adhesion Shear bond strength

Introduction

The brackets are the basis of contemporary orthodontics on which treatments are built to treat all types of malocclusions [1–5]. A proper bracket–enamel adhesion is essential to successfully complete these treatments. However the enamel–bracket interface still needs to be improved and requires further research and looking for new materials and techniques.

Despite some currently available adhesive systems can dissolve the smear layer, the most common technique used for orthodontic brackets to enamel is still the total etch adhesive using orthophosphoric acid [5, 6]. This adhesive system generates a rough area on the surface and microporosities for micromechanical retention which allows the incorporation of small resin “tags” within the enamel surface, thereby creating microscopic mechanical interlocks between the enamel and resin [7, 8]. The process provides good bond strengths but may cause decalcifications, exposing the enamel to caries attack and loss of enamel [9–12]. Because of these drawbacks, researchers look for a surface conditioner which could match the adhesive effectiveness in bracket bonding but without producing these collateral effects.

Ultrashort pulsed laser sources have attracted increasing interest for processing all kind of materials [13]. These laser pulses, amplified up to energies of the order of millijoule [14] and focused on the surface of materials, allow the ablation of thin layers with extreme precision and reproducibility, causing much less collateral damage to the adjacent material than any other thermal, chemical or mechanical process as it has been already demonstrated for dental tissues [15–22]. These outstanding features are a consequence of the nature of the interaction of such laser pulses with matter, which is based on nonlinear processes of light absorption and ionization of the material which depend mostly on the peak intensity of

the pulses followed by fast ejection due to phase explosion processes without remarkable thermal coupling with the surrounding material. This is far different from the conventional thermal ablation provided by continuous and pulsed laser sources above hundreds of picoseconds, which is based on linear absorption of the radiation, subsequent conversion of the laser energy into heat and increase of the temperature up to the vaporization point of water in the material causing explosive removal of enamel.

The total time spent in the bracket bonding is an important factor for the orthodontist in the choice of the materials and procedure for conditioning the enamel surface and the subsequent bracket adhesion. Notwithstanding the remarkable properties of ultrashort laser processing of dental tissues, processing time is probably the main bottleneck to open the orthodontic treatment to the technique. Full conditioning of one of the surfaces of a dental piece may take hours, what is unacceptable from the point of view of the clinical practice. Ultrashort laser sources with repetition rates up to tens of megahertz are available (commonly known as oscillators) but the pulses are short of energy to induce ablation of dental tissues. However, sources providing pulses with energies high enough to induce ablation at repetition rates of some hundred kilohertz have recently broken into the market. These new systems will allow reduction of the processing time in orders of magnitude, although some problems associated to heat accumulation as a result of the repetition rate may arise and should be studied. Regardless of the current and future development of laser sources with higher repetition rates, other factors affect directly the processing time and have a great influence on the adhesion properties. Namely, the geometrical features of the microstructured patterns, particularly the "density" (which accounts for the fraction of the surface that is effectively modified by laser irradiation) and the scanning speed which is at the same time limited by the pulse energy and the number of pulses needed to achieve the optimal geometry for improving the adhesion properties and to respect the integrity and mechanical properties of the original surface. Since the latter is constricted by the ablation requirements and the minimization of the collateral effects of the laser irradiation, it is the density of the microstructured pattern and its influence on the adhesion properties which is susceptible to be investigated in order to shorten the processing time. To our knowledge, there is no research focused on this issue and these studies are needed to optimize the use of this tool as an alternative to traditional conditioners in order to (1) improve bracket–enamel adhesive effectiveness, (2) minimize the problems associated to current conditioners, and (3) match or even reduce the conditioning time of the existing adhesive systems.

So far, a study of the influence of the density of ultrashort pulsed laser microstructured patterns on the shear bond strengths (SBS) of orthodontic brackets to enamel was carried out. Cross patterns with different pitches were written by ultrafast laser ablation on the surfaces of premolars that were later submitted to SBS tests, scanning electron microscope (SEM) observations, and failure mode analysis. A discussion based on the results of such analysis allows us to identify the best choice of parameters for enamel conditioning with ultrashort pulsed lasers.

Materials and methods

Sample preparation and storage

Sixty-three extracted human premolar teeth were collected and stored in a 0.5 chloramine T solution for a maximum of 6 months after extraction. Exclusion criteria included previously restored premolars and premolars with defects or cracking and delamination of the enamel.

Premolar teeth were examined with an Axio M1 light microscope (Carl Zeiss, Oberkochen, Germany) operating in the dark-field mode. Epiplan 20× and 50× HD objectives (Carl Zeiss Vision) were attached to a 1,300 × 1,030 pixel digital camera (AxioCam HR, Carl Zeiss Vision). Consistent with the exclusion criteria, the selected premolar teeth were mounted in self-cured acrylic blocks. The buccal surfaces were oriented perpendicularly to the bottom of the molds so that the bonded interfaces were parallel to the force applied during SBS tests.

Before laser irradiation, the buccal crown surface of each premolar was polished for 15 s with fluoride-free pumice slurry, washed for 30 s, and dried for 10 s with a moisture-free air spray.

Experimental groups

Prior to bonding the metal brackets, the premolar teeth were randomly assigned to nine groups, consisting of seven premolars per group, depending on the density of the laser microstructured pattern

determined by the pitch (s): (1) no laser (control), (2) $s = 15$ μm, (3) $s = 30$ μm, (4) $s = 45$ μm, (5) $s = 60$ μm, (6) $s = 90$ μm, (7) $s = 120$ μm, (8) $s = 150$ μm, and (9) $s = 180$ μm.

Ultrashort laser processing

The laser system consists of a commercial Ti:Sapphire oscillator (Tsunami; Spectra Physics, Mountain View, CA, USA) which provides pulses in the near infrared ($\lambda = 795$ nm) and a regenerative amplifier (Spitfire; Spectra Physics) based on the chirped pulse amplification technique [14] which allows to increase the pulse energy up to 1 mJ. The system delivers pulses with a duration of approximately 120 fs (1 fs = 10^{-15} s) at a repetition rate of 1 kHz and a maximum mean output power of 1 W.

The pulse energy is finely controlled by a half-wave plate and a linear polarizer. Neutral density filters were used when further energy reduction was required. The transversal mode is nearly a Gaussian TEM00 with a 9 mm beam diameter ($1/e^2$). The laser pulses were focused by means of an achromatic doublet lens ($f = 100$ mm).

The specimens were fixed on a computer-controlled XYZ motorized stage (Micos ES100; Nanotec Electronic GMBH & Co Munich, Germany). The laser pulses impinged always perpendicular to the enamel surfaces. Therefore, the optimum focalization of the pulses on the teeth surfaces was provided by Y motion and scanning by XZ motion.

For processing the enamel surfaces, a computer code was developed driving the three motors in a way that the three-dimensional surface of each premolar could be homogeneously scanned across the region of interest (ROI). Such an ROI area is in the range of 15–40 mm^2 depending on the tooth morphology. Whenever possible, we processed a larger area than bracket bases in order to ensure that adhesive deposition and bracket bonding was entirely performed within the laser-processed surface of the tooth. We have to bear in mind that the processed area in excess does not have any detrimental effect on the bonding strengths. Since the processing setup does not allow beam motion, the angle between the sample surface and the beam axis must be minimized in order to maximize the absorption of the pulse energy. Otherwise, there would be a substantial difference between the structuring at the apex and at the slopes of the surface. So far, the sample is tilted so that the laser pulses face the flatter surface possible.

The enamel was processed in tight-focusing conditions. The laser parameters were programmed according to previous works on ultrashort laser processing of hard dental tissues [15, 16]. The focal length of the lens, the pulse energy (0.03 mJ), and the scanning velocity (0.5 mm/s) were chosen to generate smoothly overlapping and swallow ablated microstructures. These parameters give a peak fluence of approximately 30 J/cm^2 (the ablation threshold fluence for enamel being 0.58 J/cm^2 [19]. With the focusing configuration used, the spot size has a diameter of approximately 12 μm ($1/e^2$), whereas the grooves generated on the surfaces are approximately 40 μm provided the ablation threshold fluence for enamel is well below $1/e^2$ times the peak fluence in our experiments.

All these parameters remain constant for all the processed specimens. The pitch between adjacent scans was gradually increased from 15 up to 180 μm generating the eight groups for further analysis as it was stated before.

The teeth samples were laser processed in a saturated vapor atmosphere to preserve the dental tissues from drying. All of the tested specimens were stored in distilled water before and after laser irradiation.

Bonding procedure

Sixty-three brackets having micro-etched bases (3M Unitek, Monrovia, CA, USA) were randomly bonded to the premolars' buccal surfaces using a total etch adhesive system to enamel consisting of a combination of a primer and an orthodontic adhesive resin (Transbond TM XT; 3M-Unitek, St. Paul, MN, US). The manufacturer's composition and application mode of the materials used in the experiment are detailed in Table 1.

Table 1 Mode of application, composition, and manufacturer of the materials

Material	Manufactured	Composition	Mode/steps of application
Transbond XT	3M ESPE, St. Paul, MN, USA	Primer: Bis-GMA, TEGDMA Adhesive paste: Silane-treated quartz, Bis-GMA, dichlorodimethylsilane reaction product with silica.	Primer: Air dry tooth thoroughly. Place small amount of Transbond XT primer in well. Apply thin uniform coat of primer on each tooth surface to be bonded. Adhesive: Aply a small bead of Transbond XT in the transfer tray. Seat the tray holding firmly in place. Cure the mesial and occlusal sides of each tube for 10 s. Scale the excess resin from around the tubes.

TEGDMA triethylene glycol-dimethacrylate, *Bis-GMA* bysphenyl glycidyl methacrylate

The adhesive resin was applied to each bracket base (area, 9.15 mm^2) after priming both the tooth and the bracket surfaces [23]. Brackets were then positioned onto the buccal enamel surfaces and pressed firmly with a Hollenback carver to expel the excess adhesive. Each bracket was subjected to a 300-g compressive force using a force gauge (Correx, Berne, Switzerland) for 10 s, after which excess bonding resin was removed using a sharp scaler. Then, the composite was light cured for 20 s from the occlusal and gingival bracket edges.

The bonding resin was photocured with a LED unit (Bluephase G2; Ivoclar-Vivadent, Schaän, Liechtenstein) emitting in the wavelength range 380–515 nm and a light intensity of 1,000 mW/cm^2 measured with a built-in radiometer (Bluephase Meter, Ivoclar-Vivadent) which was calibrated every 10 min to ensure consistent light intensity.

Shear bond strength test

The bracketed teeth were immersed in sealed containers of deionized water and placed in an incubator at 37 °C for 72 h to permit adequate water absorption and equilibration. To conduct the SBS test, the specimens were secured in a jig attached to the base plate of a universal testing machine (Autograph AGS-X 10 KN, Shimadzu, Tokyo, Japan).

The teeth were set at the base of the machine so that the sharp end of the rod incised in the area between the base and the wings of the bracket, exerting a force parallel to the tooth surface in an occluso-apical direction (crosshead speed, 0.5 mm/min). The force required to debond each bracket was registered in Newtons and converted into megapascals as a ratio of N to the bracket's surface area.

Failure mode analysis

After the SBS test, each specimen was examined with an optical microscope (Axio M1; Carl-Zeiss) at 50× magnification to identify the location of the bond failure. The adhesive layers left on the premolar surfaces were assessed by using the adhesive remnant index (ARI), where each specimen was scored according to the amount of material remaining on the enamel surface as follows: 0 = no adhesive remaining, 1 = less than 50 % of the adhesive remaining, 2 = more than 50 % of the adhesive remaining, and 3 = all adhesive remaining with a distinct impression of the bracket base.

Scanning electron microscope analysis

Three specimens per group underwent surface morphological analysis with a variable pressure SEM (Zeiss EVO MA25; Carl Zeiss, Germany). Specific regions across the surface were explored to obtain a paramount view of the effect of laser processing.

In addition, representative fractured specimens from each group were dehydrated for 48 h in a desiccator (Sample Dry Keeper Simulate Corp., Japan) and then mounted on aluminum stubs with carbon cement. They were sputter coated with 10-nm platinum layer by means of a sputter-coating Unit E500 (Polaron Equipment Ltd., Watford, UK) and then observed with the same scanning electron microscope in order to examine the morphology of the debonded interfaces.

Statistical analysis

Descriptive statistics including means and standard deviations were calculated for the SBS values. Differences in SBS among the experimental groups were examined using analysis of variance (ANOVA) and Bonferroni multiple comparisons test.

To assess the influence of the laser surface treatment on SBS, a step-wise multiple linear regression was run, the SBS being the dependent variable. The determination coefficient (R^2) was taken as the indicator of the model fit. The visualization of the relationship between SBS and pitch was performed by crossing data in a scatter plot and a quadratic regression fit plot.

The ARI scores were analyzed for percentage and frequency of fracture type, and a Chi-square test was used to match up the laser-processed groups with the control group. The ARI scores were categorized as ARI = 0–1 vs. ARI = 2–3 for statistical comparisons.

All of the statistical analyses were performed using the SPSS v.20 software for Windows (Statistical Package for the Social Sciences, Chicago, IL, USA). Significance for all statistical tests was predetermined at $p < 0.05$. Graphics were obtained by the Stata/SE v11.1 (StataCorp LP, Lakeway Drive, TX, USA).

Results

Shear bond strength

Mean values and standard deviations of SBS for the different groups are presented in Table 2. Whereas control group provides values close to those obtained in the literature, approximately 8 MPa, the laser-processed groups present much higher values. The results obtained are in the order of two and three times those of the control group, respectively, if we gather the laser-processed specimens in two families. The first one, the specimens where a cross pattern with $s > 90$ μm was performed and a second one including those processed with $s \leq 90$ μm.

Table 2. Mean and standard deviation (SD) of the shear bond strength (SBS) values (MPa) obtained among the experimental groups. ANOVA with Bonferroni correction

	Control	$s = 180$ μm	$s = 150$ μm	$s = 120$ μm	$s = 90$ μm	$s = 60$ μm	$s = 45$ μm	$s = 30$ μm	$s = 15$ μm
ANOVA $F = 7.149$ $p < 0.001$	7.8 (1.8) a	15.5 (3.3) ab	15.2 (3.2) ab	15.1 (5.1) ab	25.1 (6.0) b	24.5 (8.4) b	24.9 (3.6) b	23.6 (4.7) b	24.4 (6.7) b

Similar letters in rows indicate the absence of significant differences after Bonferroni post hoc intergroups comparisons

The ANOVA test showed that the variance of SBS within the groups was significantly discrepant ($F = 7.149$; $p < 0.001$). The Bonferroni post hoc intergroups comparisons indicated that all laser-processed groups obtained significantly higher SBS than the control group. However, $s = 120$ μm, $s = 150$ μm, and $s = 180$ μm were not significantly discrepant with regard to all the subgroups. The best adhesive performance was shown between the range 15–90 μm.

The multiple linear regression model that attempted to predict the SBS values according to the laser treatment (yes/no) and the quantitative variable "pitch" was highly significant ($F = 20.952$; $df = 2$; $p < 0.001$) and highly predictive ($R^2 = 0.50$). From this model, we observed that the intersection (representing the control group, since it is coded as laser = 0 and density = 0) has on average a SBS of 7.79 (95 % CI = 2.9–12.7 MPa), but the laser treatment significantly enhanced the SBS values (95 % CI = 12.8–24.4 MPa; $p < 0.001$). Based on the standarized coefficients, the predictor "Laser" is stronger than density of the cross pattern ($\beta = 0.79$ vs. $\beta = -0.42$, respectively), but this could be attributed to the fact that the relationship is not linear but quadratic, as it is depicted in Fig. 1, thus its influence is underestimated using a linear approach. But we have chosen the linear model for parsimonious

interpretation of the relationship and because the effect of the dichotomous variable laser treatment performs better in a linear model.

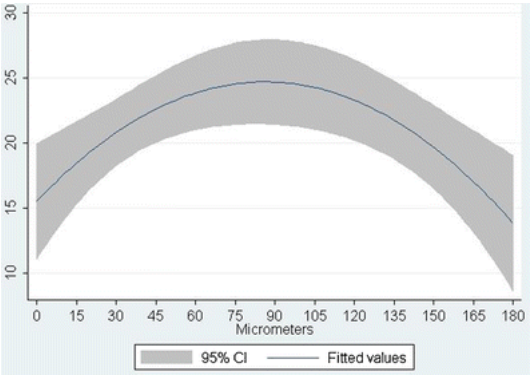

Fig. 1 Fit plot with 95 % confidence interval of the fitted values of SBS according to a cuadratic regression based only on the cross pattern pitch (*s*)

SEM observations

Representative SEM images of the enamel surface for specimens of the different groups before bonding brackets and of the debonded enamel surfaces after SBS testing are reported in Figs. 2 and 3.

Morphological analysis of laser-processed surfaces

Figure 2b–i correspond to SEM micrographs of laser-processed surfaces. Cross patterns with the desired pitches are achieved by ultrafast ablation and the ablation grooves exhibit clean and sharp edges without a recasting layer and no apparent damage to the original enamel surface beyond the limits of the microstructure. The absence of melted and scattered debris and cracks demonstrates the negligible thermal coupling of the laser pulses with the bulk material and the small influence of the propagation of shockwaves on the integrity of the enamel surface.

Since the laser parameters were not changed for the different groups, the grooves should be identical from one specimen to the others. They are approximately 40 μm wide. This can be confirmed looking at the images corresponding to the less dense patterns (Fig. 2b–f) where most of the original enamel surface was preserved. However, the smaller the pitch value the more surface is removed by laser ablation so that for a certain value of the pitch, most of the original surface has been removed (Fig. 2g–i). The shape of the processed area changes drastically, becoming a homogeneous surface some tens of microns below the raw surface of enamel and remarkably with a roughness in the micrometer range which has nothing to do with the smoothness of the original enamel surface (see Fig. 2i which corresponds to the extremal case with $s = 15$ m). Obviously, the different features of the processed surfaces for the different groups should have a relevant role on the adhesion properties.

ARI analysis

SEM micrographs of the enamel surface after debonding are shown in Fig. 3a–i. Following the criteria of Årtun y Bergland [24], we assigned an ARI value to each one of the specimens after SEM observation of the adhesion area. Table 3 shows the result of these observations grouping ARI = 0–1 and 2–3, respectively, and splitting the different laser-processed groups. In addition, Fig. 3a–i shows a micrograph of the debonded area for a representative specimen out of each group.

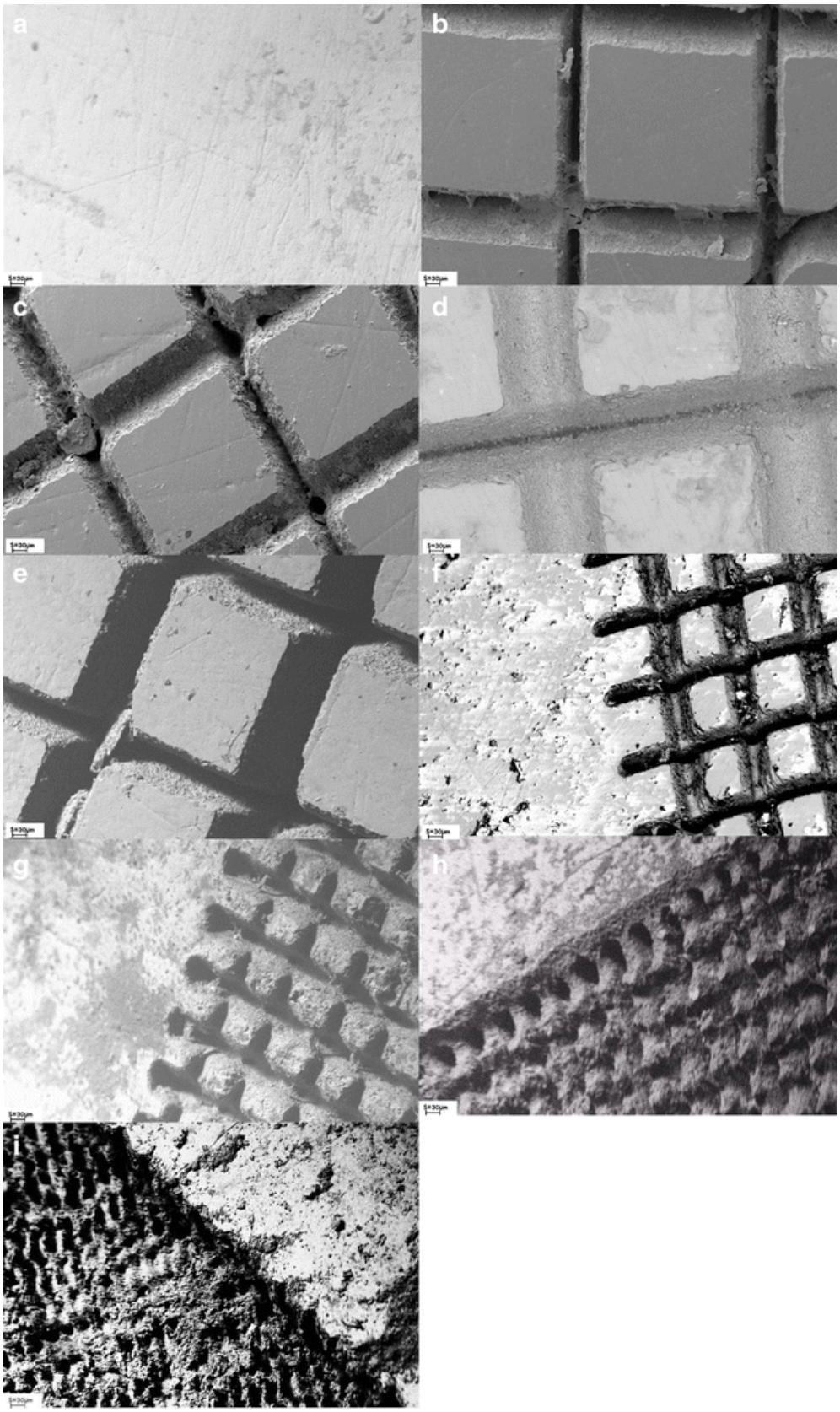

Fig. 2 SEM micrographs of enamel surface (30 μm)**. a** Control group and after ultrashort laser processing with the following pitches: **b** $s = 180$ μm, **c** $s = 150$ μm, **d** $s = 120$ μm, **e** $s = 90$ μm, **f** $s = 60$ μm, **g** $s = 45$ μm, **h** $s = 30$ μm, **i** $s = 15$ μm

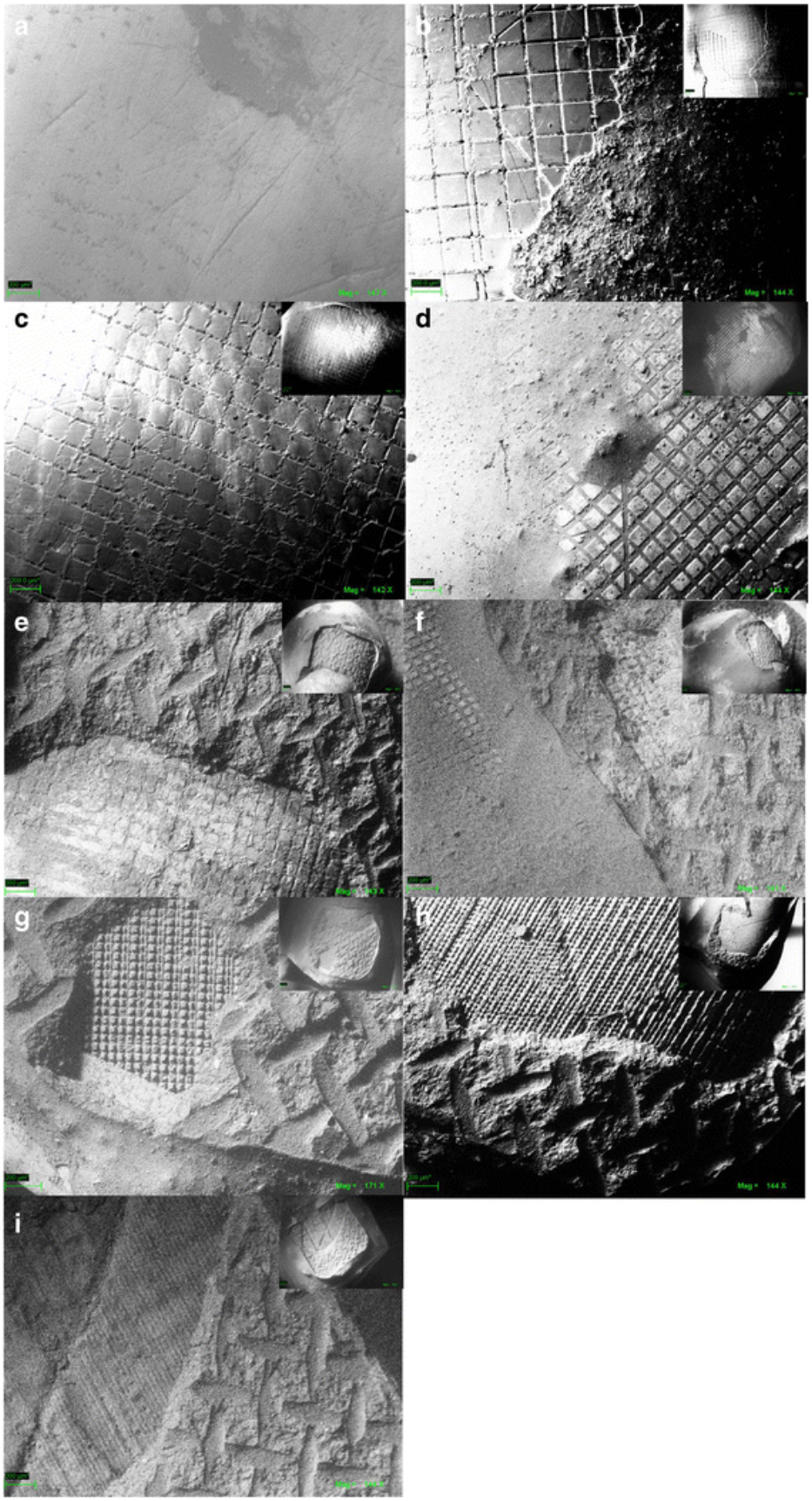

Fig. 3 SEM images of debonded specimens (200 μm). **a** Control group and laser processed **b** $s = 180$ μm, **c** $s = 150$ μm, **d** $s = 120$ μm, **e** $s = 90$ μm, **f** $s = 60$ μm, **g** $s = 45$ μm, **h** $s = 30$ μm, **i** $s = 15$ μm

Table 3 Cross-tabulation of the effect of surface treatment groups according to a dichotomous variable generated from the ARI scores (0–1 score vs. 2–3 scores). No laser subgroup was used as reference for the two-by-two comparisons

	Laser groups								
ARI	Control (%)	$s = 180$ μm (%)	$s = 150$ μm (%)	$s = 120$ μm (%)	$s = 90$ μm (%)	$s = 60$ μm (%)	$s = 45$ μm (%)	$s = 30$ μm (%)	$s = 15$ μm (%)
0–1 scores	100	100	100	100	40	0	20	0	80
2–3 scores	0	0	0	0	60	100	80	100	20
Two-by-two comparisons (no laser as reference)	a	a	a	a	B	B	B	B	a

Chi-square: 33.333 (*df*: 8); $p < 0.001$

ARI = 0 is the failure mode associated to brackets bonded directly to the raw enamel surface (Fig. 3a). The debonded surfaces do not show any residual of adhesive. The failure mode of the laser-processed specimens exhibits a behavior which is correlated to the density of the pattern. The lower the density ($s = 150$, 180 μm), the more similar is the failure mode to that of the control group (Fig. 3b, c) what is consistent with surfaces very similar to the original enamel surface. Although it is not discriminated in Table 3, the failure mode evolves to ARI = 1 as we increase the density of the pattern ($s = 120$ μm; Fig. 3d) where some of the adhesive remained on the enamel surface (but covering less than 50 % of the total surface). In the resin-free areas, the footprint of the cross pattern can be clearly observed although the grooves appear less remarkable since the adhesive has filled them.

Increasing the density of the pattern leads to failure modes which correspond mainly to ARI = 2 ($s = 60$ and 90 μm; Fig. 3e,f) and finally ARI = 3 ($s = 30$, 45 μm; Fig. 3c,d). In such cases, more than 50 % of the surface (ARI = 2) or the full surface (ARI = 3) shows the residuals of adhesive. However, a further increase of the pattern density seems to break the debonding trend. For $s = 15$ μm (Fig. 3i), the index come back to values 0–1, indicating that, concerning failure mode, the behavior of an almost fully microstructured surface resembles the enamel raw surface.

Discussion

Acid etching is routinely used in orthodontics as conditioner of the enamel surface to obtain a high bracket–enamel adhesive efficiency. However, this procedure results in chemical changes that may produce modification of the organic matter and decalcification of the inorganic component of enamel [10]. By the way, acid etching lacks selectivity and therefore the enamel surface is completely modified. In a previous study [17], it was demonstrated that ultrashort pulsed laser microstructuring of enamel surfaces could substitute acid etching as conditioning procedure as far as the SBS values obtained were comparable. As it is now well known, this laser microstructuring is very respectful with the chemical and physical properties of the original material that surrounds the processed area, specially as compared to other laser sources, avoiding almost all of the collateral effects derived from the thermal load to the material as microcracks, charring, chemical modifications, and so on [15–21, 25–27].

Nevertheless, ultrashort pulsed laser processing has a clear disadvantage as compared to acid etching as a conditioning technique. For the experiments reported in the aforementioned previous work [17], the processing took a remarkably longer time than the acid conditioning. So far, our goal in the present work was to explore how the processing parameters (in this case, the pitch of a cross pattern which was as small as 15 μm in Lorenzo et al. [17]) could affect the adhesion efficiency whereas the processing time was reduced and the largest portion of enamel surface was preserved. In Table 4, we report the average laser processing time for a complete premolar surface for the different cross patterns carried out on enamel. Since the processed surface was different for each specimen, we have estimated the time to process the minimum area (~15 mm^2). Obviously, the denser the pattern, the longer it takes to be realized.

Table 4 Average laser processing time for a complete premolar surface for the different cross patterns carried out on enamel. These times were estimated for the minimum area processed (15 mm^2)

S (microns)	15	30	45	60	90	120	150	180
T (minutes)	120	90	60	45	30	25	20	15

For the new tests, the pitch was increased from 15 μm (what we have called a very dense cross pattern) to 180 μm. We did not process with larger pitches because in those cases, the effect of the pattern on the enamel surface was almost negligible. For the specimens processed, SBS tests and SEM observations were carried out. From the SBS tests, we have observed that dense cross patterns ($s \leq 90$ μm) give rise to values three times (~25 MPa) higher than for the control group, which corresponds to raw enamel surfaces. As we increased the pitch, we found a different behavior ($s > 90$ μm); the values obtained in SBS tests decreasing to just twice (~15 MPa) those of the control group. For the latter, the portion of original enamel surface is still very large and the adhesion takes place due to the infiltration of the adhesive within the laser-processed grooves (Fig. 2b–d), which present rough walls and bottom that favor adhesion. The larger the pitch, the less original surface remains unaltered and is substituted by the laser-processed grooves (Fig. 2e–i). These surfaces foster adhesive penetration and therefore stronger bracket–enamel adhesion.

Anyway, the analysis of shear bond strengths indicates that all the specimens exhibit values beyond the clinically acceptable values (6–8 MPa) suggested by Reynolds and von Fraunhofer [28] regardless of the density of the pattern and these values are similar to those obtained with acid etching [29, 30].

In vitro studies on adhesion tests of direct bonding demonstrated that the fracture site in debonding metallic orthodontic brackets is usually located in the resin–bracket interface [31]. The ARI index provides information that has notable clinical implications for clean-up following debonding of brackets. A low ARI score implies that there is a minimal risk of iatrogenic damage to the enamel surface when residual resin composite is removed following debonding and clean-up procedures [32].

In our study, SEM observations of the failure region provide useful information (Fig. 3). We have found a clear correlation between the density of the cross pattern and the failure mode. For slightly modified surfaces, the failure mode resembles raw enamel surface behavior as expected. As we increased the density of the pattern, the ARI index evolved first to 1 (Fig. 3d) indicating that some resin is still adhered to the tooth after debonding and to 2 and 3 for $s \leq 90$ μm, when a remarkable amount of adhesive remains adhered to the specimen after debonding or the fracture takes place in the interface between resin and bracket. Finally, for extremely dense cross patterns ($s = 15$ μm), ARI values come back to 0–1. These results are consistent and compatible with the discussion concerning SBS tests. In the case of the less dense cross patterns, the surface behaves mostly as the unaltered enamel surface. As soon as we increase the density of the cross pattern, stronger adhesion induces the appearance of higher ARI scores. Finally, for the densest pattern, the bracket adheres to a surface that is no longer the original surface but an alternative surface some microns below the original one, homogeneous and much rougher than the polished enamel surface. So far, the adhesion is very strong but concerning failure, the debonding takes place uniformly all across the new surface and the result is that the remnant adhesive is scarce.

Conclusions

The introduction of an ultrashort pulsed laser cross pattern on the enamel surfaces improves bonding strengths of brackets whatever the pitch and the more the denser the pattern. Concerning the iatrogenic damage of the enamel surfaces, dense patterns lead to surfaces exhibiting large amounts of resin after debonding whereas large pitches give rise to surfaces almost free of adhesive residuals and obviously, the proportion of unaltered enamel surface is larger. With regard to time processing, since it mainly depends on scanning velocity (that was a fixed parameter in the study in order to ensure suitable ablation of enamel) and the total length of scanning for a fixed area of the specimen, it increases with the density of the pattern.

So far, although some relevant improvements in ultrashort laser technology should be expected in the near future that will shorten the time to condition the enamel surfaces for bracket bonding, up to date, the best compromise is to achieve high bond strengths, avoid excessive iatrogenic damage, and preserve a large portion of the original enamel surface is to perform cross patterns with pitches in the order of

90 μm. If the requirements concerning bond strengths are not so demanding, less dense patterns provide shorter processing times, less risk of iatrogenic damage, and an outstanding preservation of the original enamel surface.

Acknowledgments
The authors acknowledge the financial support from the Ministerio de Economía y Competitividad (projects Consolider SAUUL CSD2007-00013 and FIS2009-09522) and Junta de Castilla y León (project SA086A12-2). We are grateful to the Centro de Láseres Pulsados (CLPU, Spain) for allowing free SEM observation of the specimens.

References

1. Angle EH (1928) The latest and best in orthodontic mechanism. Dent Cosmos 70:1143–1158
2. Bishara SE, Soliman MM, Oonsombat C, Laffoon JF, Ajlouni R (2004) The effect of variation in mesh-base design on the shear bond strength of orthodontic brackets. Angle Orthod 74:400–404
3. Lugato IC, Pignatta LM, Arantes Fde M, Santos EC (2009) Comparison of the shear bond strengths of conventional mesh bases and sandblasted orthodontic bracket bases. Braz Oral Res 23:407–414
4. Kang DY, Choi SH, Cha JY, Hwang CJ (2013) Quantitative analysis of mechanically retentive ceramic bracket base surfaces with a three-dimensional imaging system. Angle Orthod 83(4):705–711
5. Türköz C, Ulusoy C (2012) Evaluation of different enamel conditioning techniques for orthodontic bonding. Korean J Orthod 42:32–38
6. Schnebel B, Mateer S, Maganzini AL, Freeman K (2012) Clinical acceptability of two self-etch adhesive resins for the bonding of orthodontic brackets to enamel. J Orthod 39:256–261
7. Gwinnett AJ, Matsui A (1967) A study of enamel adhesives. The physical relationship between enamel and adhesive. Arch Oral Biol 12:1615–1620
8. Buonocore MG, Matsui A, Gwinnett AJ (1968) Penetration of resin dental materials into enamel surfaces with reference to bonding. Arch Oral Biol 13:61–70
9. Buonocuore MG (1955) A simple method of increasing the adhesion of acrylic filling materials to enamel surfaces. J Dent Res 34:849–853
10. Pashley DH (1992) The effects of acid etching on the pulpodentin complex. Oper Dent 17:229–242
11. Lehman R, Davidson CL (1981) Loss of surface enamel after acid etching procedures and its relation to fluoride content. Am J Orthod 80:73–82
12. Shey Z, Brandt S (1982) Enamel loss due to acid treatment for bonding. J Clin Orthod 16:338–340
13. Moulton PF (1986) Spectroscopic and laser characteristics of Ti:Al2O3. J Opt Soc Am B 3:125–133
14. Strickland D, Mourou G (1985) Compression of amplified chirped optical pulses. Opt Commun 56:219–221
15. Portillo Muñoz M, Lorenzo Luengo MC, Sánchez Llorente JM, Peix Sánchez M, Albaladejo A, García A, Moreno Pedraz P (2012) Morphological alterations in dentine after mechanical treatment and ultrashort pulse laser irradiation. Lasers Med Sci 27:53–58
16. Luengo MC, Portillo M, Sánchez JM, Peix M, Moreno P, García A, Montero J, Albaladejo A (2013) Evaluation of micromorphological changes in tooth enamel after mechanical and ultrafast laser preparation of surface cavities. Lasers Med Sci 28:267–273
17. Lorenzo MC, Portillo M, Moreno P, Montero J, Castillo-Oyagüe R, García A, Albaladejo A (2013) In vitro analysis of femtosecond laser as an alternative to acid etching for achieving suitable bond strength of brackets to human enamel. Lasers Med Sci. doi:10.1007/s10103-013-1278-5
18. Portillo M, Lorenzo MC, Moreno P, García A, Montero J, Ceballos L, Fuentes MV, Albaladejo A (2013) Influence of Er:YAG and Ti:sapphire laser irradiation on the microtensile bond strength of several adhesives to dentin. Lasers Med Sci. doi:10.1007/s10103-013-1343-0
19. Ji L, Li L, Devlin H, Liu Z, Jiao J, Whitehead D (2012) Ti:sapphire femtosecond laser ablation of dental enamel, dentine, and cementum. Lasers Med Sci 27:197–204
20. Rego Filho Fde A, Dutra-Corrêa M, Nicolodelli G, Bagnato VS, de Araujo MT (2013) Influence of the hydration state on the ultrashort laser ablation of dental hard tissues. Lasers Med Sci 28(1):215–222
21. Schelle F, Polz S, Haloui H, Braun A, Dehn C, Frentzen M, Meister J (2013) Ultrashort pulsed laser (USPL) application in dentistry: basic investigations of ablation rates and thresholds on oral hard tissue and restorative materials. Lasers Med Sci (in press)
22. Braun A, Krillke RF, Frentzen M, Bourauel C, Stark H, Schelle F (2013) Heat generation caused by ablation of dental hard tissues with an ultrashort pulse laser (USPL) system. Lasers Med Sci (in press)
23. Goracci C, Margvelashvili M, Giovannetti A, Vichi A, Ferrari M (2013) Shear bond strength of orthodontic brackets bonded with a new self-adhering flowable resin composite. Clin Oral Investig 17:609–617
24. Årtun J, Bergland S (1984) Clinical trials with cristal growth conditioning as an alternative to acid-etch enamel pretreatment. Am J Orthod 85:333–340
25. Hibst R, Keller U (1989) Experimental studies of the application of the Er:YAG laser on dental hard substances: I. Measurement of the ablation rate. Lasers Surg Med 9:338–344

26. Walsh LJ, Perham SJ (1991) Enamel fusion using a carbon dioxide laser: a technique for sealing pits and fissures. Clin Prev Dent 13:16–20
27. Altundasar E, Ozçelik B, Cehreli ZC, Matsumoto K (2006) Ultramorphological and histochemical changes after ER, CR:YSGG laser irradiation and two different irrigation regimes. J Endod 32:465–468
28. Reynolds IR, von Fraunhofer JA (1976) Direct bonding of orthodontic attachments to teeth: the relation of adhesive bond strength to gauge mesh size. Br J Orthod 3:91–95
29. Başaran G, Hamamcı N, Akkurt A (2010) Shear bond strength of bonding to enamel with different laser irradiation distances. Lasers Med Sci 26:149–156
30. Scougall Vilchis RJ, Yamamoto S, Kitai N, Yamamoto K (2009) Shear bond strength of orthodontic brackets bonded with different self-etching adhesives. Am J Orthod Dentofacial Orthop 136:425–430
31. Keizer S, Ten Cate JM, Arends J (1976) Direct bonding of orthodontic brackets. Am J Orthod 69:318–327
32. Zarrinnia K, Eid NM, Kehoe MJ (1995) The effect of different debonding techniques on the enamel surface: an in vitro qualitative study. Am J Orthod Dentofac Orthop 108:284–293